Solid State Communications 154 (2013) 72–76

Contents lists available at SciVerse ScienceDirect

Solid State Communications

journal homepage: www.elsevier.com/locate/ssc

Pressure induced phase transitions in multiferroic $BiFeO_3$

A.K. Mishra [a,*], K.V. Shanavas [a,1], H.K. Poswal [a], B.P. Mandal [b], Nandini Garg [a], Surinder M Sharma [a]

[a] High Pressure and Synchrotron Radiation Physics Division, Bhabha Atomic Research Centre, Trombay, Mumbai 400085, India
[b] Chemistry Division, Bhabha Atomic Research Centre, Trombay, Mumbai 400085, India

ARTICLE INFO

Article history:
Received 28 September 2012
Accepted 14 October 2012
by A.H. MacDonald
Available online 24 October 2012

Keywords:
A. Multiferroic
E. High pressure
E. X-ray diffraction
E. First principles

ABSTRACT

Using synchrotron based angle dispersive x-ray diffraction measurements and first principles calculations we have studied the high pressure behavior of pervoskite $BiFeO_3$. We report two structural phase transitions under pressure viz., at ~4.1 and ~6.4 GPa. Our first principles calculations, combined with Rietveld refinement of the diffraction data, suggest that both the high pressure phases are orthorhombic, the first being $P222_1$ and the second phase belonging to the space group Pnma. These results are in contrast to the previous studies such as the observation of monoclinic phase below 10 GPa. Theoretical structural optimization in the present case indicates the utility of incorporating the chemical bonding in Rietveld refinement of complex structures.

1. Introduction

Cubic perovskites undergo structural phase transitions by distortion/rotation of octahedral and/or movement of the central cation, driven by Jahn–Teller distortions. Several of these also display ferroelectric or ferroelastic instabilities leading to multiferroicity. These novel properties are exploited in the usage of these materials in the field of data storage, microelectronic devices, spintronics etc. [1,2]. The distortions are expected to diminish on increase of temperature, as the structure tends towards the parent perovskite form [3]. Effects of pressure on structure, however, are difficult to predict due to the complex changes in the inter-ionic interactions coupled with the interplay of several degrees of freedom such as distortion/rotation of octahedra, displacement of ions etc.

Bismuth ferrite ($BiFeO_3$) is a multiferroic in which the ferroelectricity arises due to the 6*s* lone pair electrons of bismuth, [4–6], and the partially filled *d* orbitals of Fe generate the magnetic ordering. At room temperature $BiFeO_3$ crystallizes into rhombohedrally distorted perovskites with space group R3c [7,8]. This structure is derived from cubic Pm $\bar{3}$m structure by displacement of Fe^{3+} and Bi^{3+} cations from their centro-symmetric positions along [111] pseudo cubic direction and an antiphase tilting of the adjacent FeO_6 octahedra. It is one of the few perovskites which exhibits both the displacement of the cations from their centro-symmetric position as well as the tilt of the octahedra.

The high pressure behavior of $BiFeO_3$ has earlier been investigated by several groups and has led to a multitude of, sometimes contradictory, observations [9–16]. In one of the earliest studies, using Raman scattering and Ar as pressure transmitting medium (PTM), Haumont et al. [9] reported two high pressure phase transitions at ~3.5 GPa and ~10 GPa to C2/m and Pnma respectively. These were later confirmed by them with x-ray diffraction (XRD) measurements employing a more hydrostatic (hydrogen) PTM [10]. However, XRD experiments by Gavriliuk et al. [11], using PTM like hydrogen and helium, did not show any transition till 50 GPa, at which pressure $BiFeO_3$ underwent a Mott transition to a metallic phase. Subsequent XRD experiments [12] reported a single transition, but at 10 GPa. In contrast Belik et al. [13] claimed the observation of three structural transitions (using the 16:4:1 methanol:ethanol:water (M:E:W) mixture as PTM) viz., R3c→orthorhombic1→orthorhombic2→Pnma. In fact Belik et al. also discussed the presence of an Orthorhombic3 phase on release of pressure. However, it should be noted that the samples used by these authors had impurities arising from the unreacted and intermediate reaction products. Measurements carried out on single crystals of $BiFeO_3$ by Guenno et al. [14] suggest that under hydrostatic conditions there are two intermediate phases while under non-hydrostatic conditions there are three phases. However, these authors did not report the crystal structures of the high pressure phases.

Theoretical results are also similarly diverse: ab-initio calculations by Ravindran et al. [15] indicated that $BiFeO_3$ transforms to the Pnma phase at 10 GPa. However, corroborating the results of Gavriliuk et al., ab initio calculations of Vazquez et al. [16] also

* Corresponding author. Tel.: +91 22 25591312; fax: +91 22 25505296.
E-mail address: akmishra@barc.gov.in (A.K. Mishra).
[1] Present Address: Department of Physics and Astronomy, University of Missouri, Columbia, MO 65211, USA.

0038-1098/$ - see front matter © 2012 Elsevier Ltd. All rights reserved.
http://dx.doi.org/10.1016/j.ssc.2012.10.018

showed that $BiFeO_3$ undergoes a first order phase transition from a high spin (Fe^{3+}) state phase to a low spin (Fe^{3+}) state phase at 36 GPa. Recently, using first principles methods, Dieguez et al. [17] have performed a systematic search for the potentially stable phases of $BiFeO_3$ and found a large number of possibly competing structures.

These studies suggest that structural determination for $BiFeO_3$ using only diffraction data may not be unambiguous as the refinement programs generally do not factor in the energetics implications of changes in the chemical bonds. Hence to determine the structure of the intermediate phase in this compound we have carried out high pressure x-ray diffraction studies in combination with first principles ab-initio study on $BiFeO_3$. We have tried to interweave the results from both these studies to solve the structure of the intermediate high pressure phase.

2. Experimental details

Equimolar amounts of $Bi(NO_3)_3$ and $Fe(NO_3)_3$ were dissolved in 2N HNO_3 along with tartaric acid in 1:1 M ratio with respect to the metal ion. This solution was heated under constant stirring at 200 °C till all the liquids evaporated. Finally this dry powder was calcined at 500 °C for about half an hour to yield $BiFeO_3$. This sample was characterized with the help of x-ray diffraction. Rietveld refinement of this data confirms the formation of rhombohedral (S.G. R3c) $BiFeO_3$ and a small amount of (2% in weight) $Bi_2Fe_4O_9$ impurity. The unit-cell parameters were determined to be $a=5.571(1)$ Å and $c=13.827$ (3) Å (hexagonal setting), which are in good agreement with the earlier reported lattice constants of $BiFeO_3$ [18,19].

For high pressure experiments finely powdered sample of $BiFeO_3$ was loaded along with a few specs of copper in a hole, of ~100 μm diameter, drilled in a pre indented (~70 μm thick) tungsten gasket of a diamond-anvil cell (DAC). Methanol: ethanol (4:1) mixture was used as pressure transmitting medium. The pressure was determined from the known equation of state of copper [20]. High-pressure angle dispersive x-ray-diffraction experiments ($\lambda=0.68881$ Å), were carried out up to~27.0 GPa at the 5.2 *R* (*XRD1*) beamline of Elettra Synchrotron source. The diffraction patterns were recorded using MAR345 imaging plate detector kept at a distance of ~20 cm from the sample. Two-dimensional x-ray diffraction patterns were transformed to one-dimensional diffraction profiles by the radial integration of diffraction rings using the FIT2D software [21].

3. First principles method

Electronic structure calculations were carried out using VASP code [22] with local density approximation for the exchange correlation and plane augmented wave [23,24] method to approximate the core electrons. A kinetic energy cutoff of 400 eV and Monkhorst Pack *k*-point grid of $9\times9\times9$ was found sufficient to ensure convergence. The lattice constants and fractional coordinates of the different high pressure phases determined from experiments were used as the starting structures for the simulations.

Complete ionic relaxation was carried out at various volumes in anti-ferromagnetic spin arrangement to find the lowest energy configurations. For this, symmetry and volume of the simulation box was fixed and the ionic degrees of freedom were allowed to relax to the minimum energy configurations.

4. Results and discussion

The x-ray diffraction pattern of $BiFeO_3$ at a few representative pressures is shown in Fig. 1.

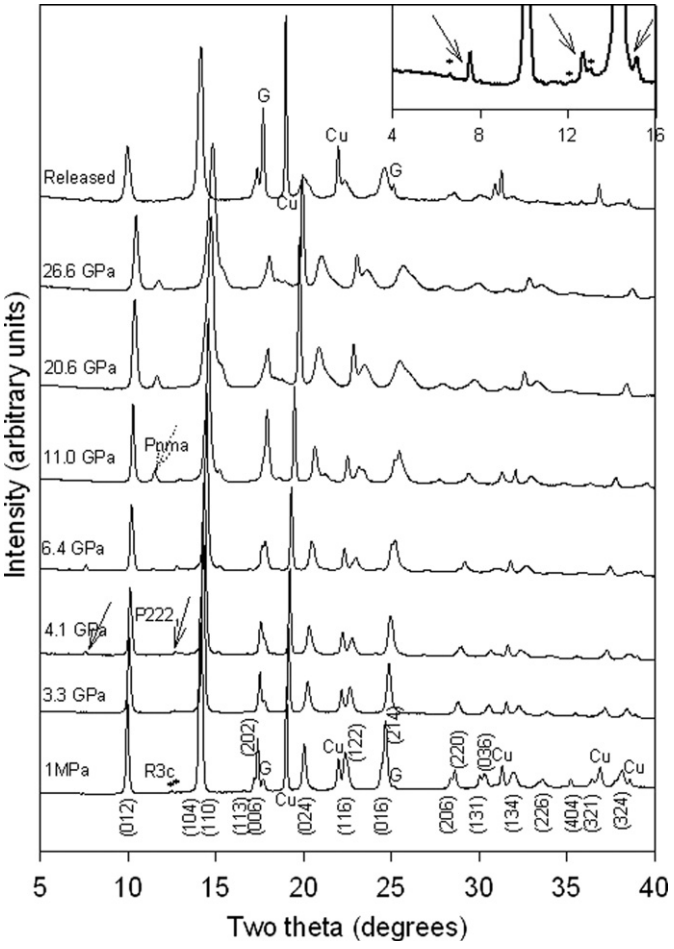

Fig. 1. X-ray diffraction pattern of $BiFeO_3$ at a few representative pressures. X-ray diffraction peaks marked with the star are from impurity while the peaks marked with solid and dotted arrows are from the new high pressure phases with space group $P222_1$ and Pnma respectively. The inset shows the zoomed view of diffraction pattern at 4.1 GPa and highlights the fact that the new XRD peaks of $P222_1$ phase are distinct from the impurity peaks.

The impurity peaks are very weak and have been marked with a star. These peaks can be followed upto 3 GPa beyond which they are not discernible. The appearance of new weak peaks in the diffraction pattern at 4.1 GPa indicate that $BiFeO_3$ has undergone a structural phase transition to a lower symmetry phase. Inset shows that these new peaks are distinct from the impurity peaks. The diffraction pattern appears to be similar to the first high pressure phase observed by Haumont et al. [8]. On comparing the 7.5 GPa diffraction pattern of Gavriliuk et al. we find that very weak diffraction peaks ignored by these authors actually have 'd' spacings (at 5.21 Å, 3.1 Å, 2.61 Å) similar to those of the new peaks observed by us and Haumont et al. [8]. Since the new diffraction peaks are very weak the authors might have missed these new peaks, concluding the absence of any phase change upto 50 GPa. We have observed that in our studies these diffraction peaks remain weak over the entire range of existence implying that the first high pressure phase may not be very different from the initial phase and could be obtained by a slight distortion of the R3C structure. On further increase of pressure new weak diffraction peaks start appearing at 6.4 GPa indicating the onset of a second phase transition. By 11 GPa the transformation seems to be complete as the new peaks become stronger and some of the diffraction peaks of the first high pressure phase have disappeared. Coexistence of both the high pressure phases over this pressure range implies the first order nature of this

transformation. On release of pressure the diffraction pattern of the initial phase was retrieved indicating the reversibility of both the phase transitions.

The structure of the second high pressure phase at 11 GPa was found to be similar to that reported in earlier experiments (orthorhombic non-polar Pnma). However, to determine the structure of the first high pressure phase observed at 4.1 GPa we fitted all the diffraction peaks and determined their peak positions. Eighteen XRD peaks were used to determine the structure of the new phase with the help of the CRYSFIRE package [25]. An orthorhombic cell was fitted with a figure of merit 6.1. Using the extinction conditions in CHECKCELL [26] the most probable space group of the first high pressure phase was determined to be $P222_1$ (S.G. no.17). From density considerations this first high pressure phase should have at least 8 formula units, compared to 6 in the ambient R3C phase. Using the reverse Monte Carlo method (FOX software) an approximate structure was determined for the first high pressure phase. Using the information so derived, we carried out Rietveld analysis using the GSAS software. The goodness of fit parameters were $R_{wp}=6.5\%$, $R_p=4.8\%$ with a reduced $\chi^2=0.413$. However, after the final refinement we found that the structure was very strained with some of the Fe–O distances as short as 1.696 Å compared to 2.1 Å and 1.9 Å at ambient pressures.

In addition to orthorhombic ($P222_1$) we have also considered monoclinic (C2/m) structure of Ref [8] as a possible candidate. The monoclinic structure consists of 12 formula units per units cell and even for this structure a large variation in the Bi–O (1.76 Å–2.5 Å) and Fe–O (1.24 Å–2.13 Å) bond lengths was observed. This type of a bond length distribution appears to be unphysical for this compound. On refinement we found that despite the larger number of refinable parameters, the measures of goodness of fit were poorer ($R_{wp}=10\%$, $R_p=7\%$ with reduced $\chi^2=1.1$) compared to those of $P222_1$.

Although fit with the orthorhombic structure is better than the monoclinic, both structures are significantly strained at the end of refinement. To fix this, we have used first principles based structural optimization technique to let the atomic coordinates evolve to minimize the local forces. Accordingly, starting from the experimentally obtained structural parameters, we have optimized the coordinates in R3c, $P222_1$ and C2/m phases at different volumes. As expected, at higher volumes (or lower pressures), the rhombohedral R3c phase is found to be energetically stable. The initial orthorhombic ($P222_1$) and monoclinic (C2/m) structure were also relaxed using first principles calculations. Fig. 2 shows the nature of changes brought about by these simulations on both the structures.

We used both of these optimized structures for the final Rietveld refinement. The fit was found to be much better in the case of the $P222_1$ phase and has been shown in Fig. 3. The goodness of fit parameters were found to be $R_{wp}=6.1\%$, $R_p=4.4\%$, and reduced $\chi^2=0.414$. As mentioned above, even with the relaxed coordinates the fit of the C2/m phase was poorer than that of the $P222_1$ phase with goodness of fit parameters, $R_{wp}=8.7\%$, $R_p=6.4\%$, and reduced $\chi^2=0.85$. Hence, we conclude that the first high pressure phase belongs to $P222_1$ orthorhombic structure. The fractional coordinates of the refined $P222_1$ phase and Pnma phase have been given in Table 1 and Table 2 respectively.

Since the main diffraction peaks of all the phases from R3C to Pnma are similar we would expect small distortions and tilts to bring about these phase transitions. This can be clearly seen from Fig. 4 where we have plotted all the three structures.

It can be seen that on increase of pressure the octahedra rotate about 'b' axis of the ambient phase, with a slight shift of the Fe atoms towards the centre of symmetry. Our studies along with the earlier reports suggest that irrespective of the PTM at least one high pressure phase is observed between the ambient and the Pnma phase.

The pressure induced variation of volume per formula unit of the three phases is shown in Fig. 5. On fitting the third order Birch–Murnaghan equation of state [27] to all the three phases we found

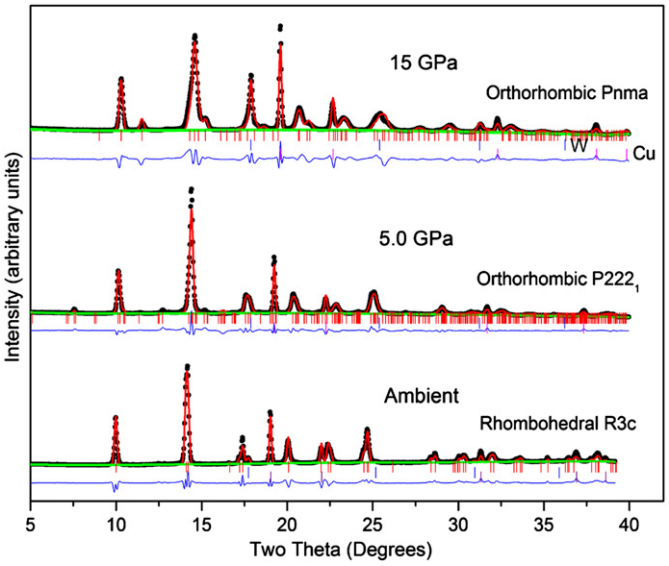

Fig. 3. Rietveld refined diffraction pattern of $BiFeO_3$ at three different pressures (ambient, 5.0 GPa and 15.0 GPa) representing Rhombohedral (R3c), Orthorhombic ($P222_1$) and (Pnma) symmetries respectively. For Rietveld refinement three contributions viz. from BiFeO3, tungsten (gasket) and copper (the pressure marker) were used at each pressure. The red, green and blue solid lines represent the calculated intensity, background and difference from observed data respectively while the black dots represent the experimental data. (For interpretation of the references to color in this figure legend, the reader is referred to the web version of this article.)

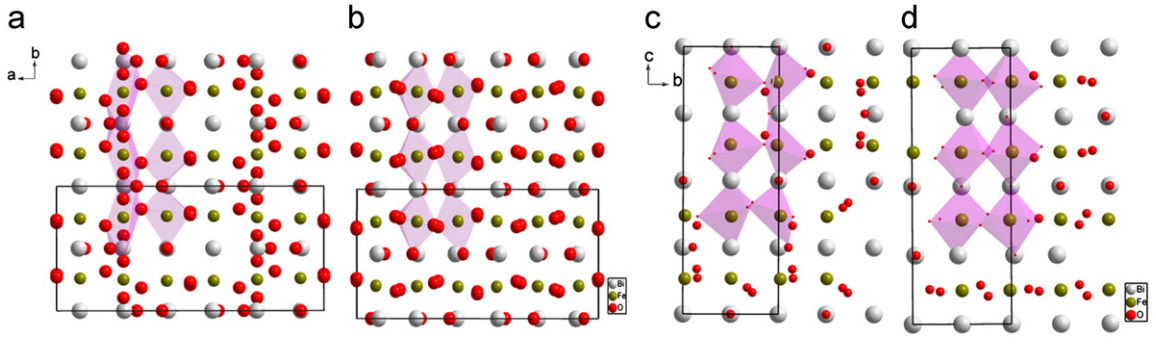

Fig. 2. (a) Rietveld refined monoclinic (C2/m) structure (from reference 8).(b) Relaxed monoclinic structure after theoretical structural optimization (present study). The resulting bond lengths for Bi–O and Fe–O changed from 2.22 Å to 2.44 Å and 1.86 Å to 1.89 Å respectively (c) Rietveld refined orthorhombic ($P222_1$) structure (present study, without relaxation). (d) Relaxed orthorhombic ($P222_1$) structure after theoretical structural optimization.

that the bulk moduli are as follows: R3c — 105.9 ± 1.2 GPa, $P222_1$— 110.5 ± 3.1 GPa, Pnma — 305.4 ± 5.8 GPa. The pressure derivative was fixed to be 4 in all the three cases. From these results we can see that the R3c and $P222_1$ phases have similar compressibility in contrast to the non polar Pnma phase which is relatively incompressible. The bulk modulus of the R3c phase is in close agreement with earlier determined values of 111 GPa [10] and 97 GPa [12] respectively. However, using the PV data up to 40 GPa, Gavriliuk et al. [11] determined the bulk modulus of the R3c phase to be 75.5 GPa. Bulk modulus of Pnma phase determined by us is in agreement with earlier studies [11,12]. The enhanced bulk modulus of Pnma phase is indicative of change in the nature of bonding of $BiFeO_3$ under pressure.

5. Conclusion

Usually determination of the structure of the high pressure phases is a challenging task as the data is limited and there may be competing solutions. If the initial model structure is not close to the actual structure, Rietveld method may give somewhat unrealistic structures such as the structures with strained bonds. This is because this method essentially minimizes the disagreement which might lead it to a local minimum and not the global minimum. However, if one uses a combination of Rietveld refinement along with first principles based structure relaxation (using minimization of interatomic forces) one is more likely to get to the global minimum and thus closer to a real structure.

Using this methodology we have concluded that $BiFeO_3$ undergoes two phase transitions viz., at 4.1 GPa and 6.4 GPa to orthorhombic phases $P222_1$ and Pnma respectively. The first high pressure phase has compressibility similar to that of the ambient

Table 1
Fractional coordinates of orthorhombic phase ($P222_1$) at 4.1 GPa (First high pressure phase).

$a=5.4858$ Å, $b=5.5577$ Å and $c=14.4582$ Å with $Z=8$			
	x	y	z
Bi	0	0.46262	1/4
Bi	1/2	0.02891	1/4
Bi	1/2	0	0
Bi	0.95900	1/2	0
Fe	−0.01780	−0.01470	0.37770
Fe	0.51640	0.50110	0.37830
O1	0.67370	0.82600	0.62610
O2	0.18640	0.72040	0.61790
O3	0.72720	0.76430	0.10100
O4	0.80220	0.68800	0.35900
O5	0	0.03860	1/4
O6	1/2	0.43490	1/4
O7	0.06450	0	0
O8	0.45380	1/2	0

Table 2
Fractional coordinates of orthorhombic phase (Pnma) at 11 GPa (2nd high pressure phase).

$a=5.531$ Å, $b=7.687$ Å, $c=5.359$ Å with $Z=4$			
	x	y	z
Bi	0.55360	0.25000	0.51140
Fe	0.00000	0.00000	0.50000
O	0.53341	0.25000	0.10360
O	0.20000	0.95400	0.19450

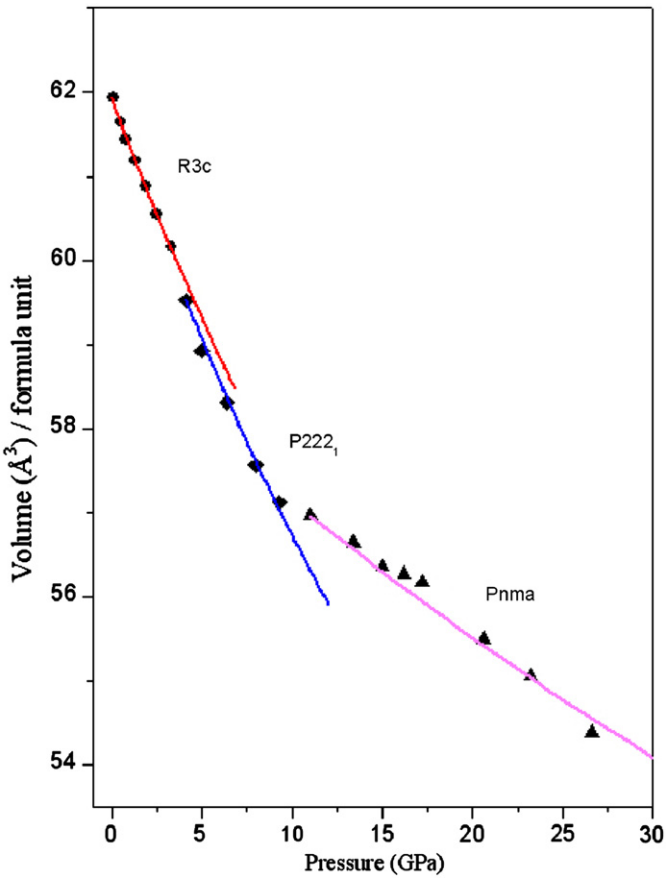

Fig. 5. Observed variation in the volume (per formula unit) of $BiFeO_3$ as a function of pressure. Symbols represent the experimentally observed data while solid lines are obtained from fitting the P-V data with third order Birch–Murnaghan equation of state.

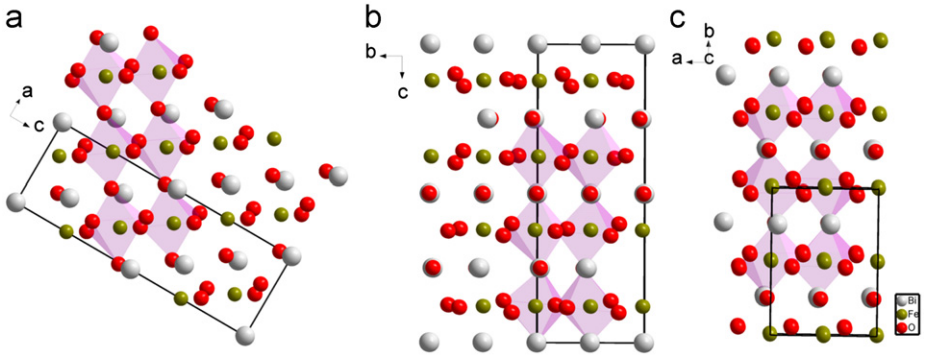

Fig. 4. (a) Crystal structure of $BiFeO_3$ at ambient conditions. (b) The structure of the first high pressure phase ($P222_1$). (c) Structure of the second high pressure phase (Pnma).

phase while the second high pressure phase becomes significantly less compressible.

References

[1] Y. Tokura, Science 312 (2006) 1481.
[2] M. Bibes, A. Barthelemy, Nat. Mat 7 (2008) 425.
[3] C.J. Howard, H.T. Stokes, Acta Cryst. A 61 (2005) 93.
[4] N.A. Spaldon, J. Phys. Chem. B 104 (2000) 6694.
[5] R. Ramesh, N.A. Spaldon, Nat. Mater. 6 (2007) 21.
[6] S.W. Cheong, M. Mostovoy, Nat. Mater. 6 (2007) 13.
[7] P. Fischer, M. Polomska, I. Sosnowska, M. Szymanski, J. Phys. C 13 (1980) 1931.
[8] F. Kubel, H. Schmid, Acta Crystallogr. Sect. B: Struct. Sci 46 (1990) 698.
[9] R. Haumont, J. Kreisel, P. Bouvier, Phase Transit. 79 (2006) 1043.
[10] R. Haumont, P. Bouvier, A. Pashkin, K. Rabia, S. frank, B. Dkhil, W.A. Crichton, C.A. Kuntscher, j. Kreisel, Phys. Rev. B 79 (2009) 184110.
[11] A.G. Gavriliuk, V.V. Struzhkin, I.S. Lyubutin, S.G. Ovchinnokov, M.Y. Hu, P. Chow, Phys. Rev. B 77 (2008) 15512.
[12] J.L. Zhu, S.M. Feng, L.J. Wang, C.Q. Jin, X.H. Wang, L.T. Li, Y.C. Li, X.D. Li, J. Liu, High Press. Res 30 (2010) 265.
[13] A.A. Belik, H. Yusa, N. Hirao, Y. Ohishi, E. Takayama-Muromachi, Chem. Mater. 21 (14) (2009) 3400.
[14] M. Guennon, P. Bouvier, r. Haumont, G. Garbarino, J. Kriesel, Phase Transit 84 (2011) 474.
[15] P. Ravindran, R. Vidya, A. Kjekshus, H. Fjellvag, O. Eriksson, Phys. Rev. B. 74 (2006) 224412.
[16] O.E.G. Vazquez, J. Iniguez, Phys. Rev. B 79 (2009) 064102.
[17] O. Dieguez, O.E. Gonzalez-Vazquez, J.C. Wojdel, J. Iniguez, Phys. Rev. B 83 (2011) 094105.
[18] F. Kubel, H. Schmid, Acta Crystallogr. Sect. B: Struct. Sci 46 (1990) 698.
[19] J.D. Bucci, B.K. Robertson, W.J. James, J. Appl. Crystallogr 5 (1972) 187.
[20] Dewaele, P. Loubeyre, M. Mezouar, Phys. Rev. B 70 (2004) 094112.
[21] P. Hamersley, S.O. Svensson, M. Hanfland, A.N. Fitch, D. Hauserman, High Press. Res 14 (1996) 235.
[22] G. Kresse, J. Hafner, Phys. Rev. B 47 (558) (1993);
G. Kresse, J. Furthümller, Phys. Rev. B 54 (1996) 11169.
[23] P.E. Blochl, Phys. Rev. B 50 (1994) 17953.
[24] G. Kresse, D. Joubert, Phys. Rev. B 59 (1999) 1758.
[25] R. Shirley, The Crysfire System for Automatic Powder Indexing (The Lattice, Surrey UK 1999).
[26] J. Laugier, B. Bochu, 〈http://www.ccp14.ac.uk/tutorial/Imgp〉.
[27] F. Birch, J. Geophys. Res. 83 (1978) 1257.